2015 Workshop on Research, Education and Development of
Unmanned Aerial Systems (RED-UAS)
November 23-25, 2015. Cancun, Mexico

PID-based fail-safe strategy against the break of opposite motors in quadcopters

Raif C. Gomes, George A. P. Thé
Depto. de Engenharia de Teleinformática
Universidade Federal do Ceará
Fortaleza, Brazil
Email: raif.carneiro@gmail.com,george.the@ufc.br

***Abstract*—The growing interest on service robotics with the use and exploitation of unmanned aerial vehicles has revealed important issues related to safety and fail prevention during navigation, and recent research has been devoted to understand and modeling the breaking of 1, 2 or even 3 motors. In this context, the present paper investigates the dynamics of an unmanned aerial vehicle of quadrotor type using PID controllers before a scenario of total failure in two opposite engines and analyses the existing relation between an equipment design issue and its navigation condition after such a failure. As a contribution, it is proposed and discussed from simulations a strategy to mitigate the mentioned failure by landing the quadrotor in a smoothly fashion. At last, preliminary results of a real failure scenario are shown to match simulated predictions.**

***Keywords*-Unmanned aerial vehicles, PID controller, fail-safe navigation**

I. Introduction

The recent progress of the microelectronic industry with the offer of microelectromechanical sensors (MEMS), as well as that of chemicals, with the availability of efficient batteries has led to significant diffusion of robots in different domains, far beyond the industrial shop floor. It gave rise to service robotics, which, already in 2012 was defined by the International Federation of Robotics as the field comprising robots able to perform useful tasks for man or machines, excluded industrial automation applications. In this context, in the last decade the unmanned aerial vehicles (UAV) attracted a lot of attention for the potential use in military missions, as well as for the wide range of commercial applications they can be used in [1].

Until the present days, use and public exploitation of UAVs requires regulation, maybe due to relevant but still open issues, which are normally taken into account in engineering products design; one example is people safety before failure of those equipments. As a matter of fact, the growing interest in service robotics has pushed on the design of critical safety systems [2], especially towards the deployment of on-navigation fail-safe controllers.

This issue is a hot topic in the recent literature. While part of the scientific community is interested in the partial loss of motor efficiency [3], other recent papers considered the complete breaking of 1, 2 and/or even 3 motors of the vehicle. This is the case presented in [4], in which the flight stabilization is investigated theoretically and experimentally, as well. In [5], in turn, authors focus on the flight stabilization again, but for the case of 1 motor loss only.

Most of those works deal with the design of a controller able to guarantee safe navigation conditions after a failure rises. Essentially, the appearance of breaking signs the transition between a cascade configuration of PID controllers (to be discussed) and the use of what is hereafter named critical controller (able to ensure fail-safety).

A deep reading of the recent bibliography reveals that the PID strategy is often neglected as a choice for the critical controller. In our comprehension, however, this deserves a discussion, since the PID is by far the most used closed-loop control approach and do not pose difficulties for hardware implementation.

A second issue which is considered here is the influence of the UAV geometrical design on its navigation condition. From time-domain dynamical simulations, we will discuss how the drag coefficient affects the stability of a quadrotor under failure in two propellers.

This work is organized as it follows: section II describes the basic dynamic equations of movement for a quadrotor, whereas in section III details about the adopted non-critical controller are given. Section IV, in turn, brings basic simulation results of a positioning task under a small-variation approximation of the orientation angles. Section V considers the breaking of two motors and proposes a fail-safe technique. In the section VI preliminary results of a real failure scenario are shown. Finally, in section VII conclusions are drawn and in section VIII futures works are described.

II. Dynamics of a quadrotor

Essentially, in a very common configuration a quadrotor is a crossed structure of rods having rotating wings driven by 4 engines at the corners, as illustrated in Figure 1.

By controlling the speed and the rotation sense of every motor, the vehicle can rotate over the three spatial directions, giving rise to three very characteristics angles: yaw (ψ), pitch (ϕ) and roll (θ). Control of pitch and roll angles leads to translational displacement, whereas the control of yaw

Fig. 1: Home-mounted quadrotor based on open technology.

angle is related to circular movement (around the z-axis), as illustrated in Figure 2.

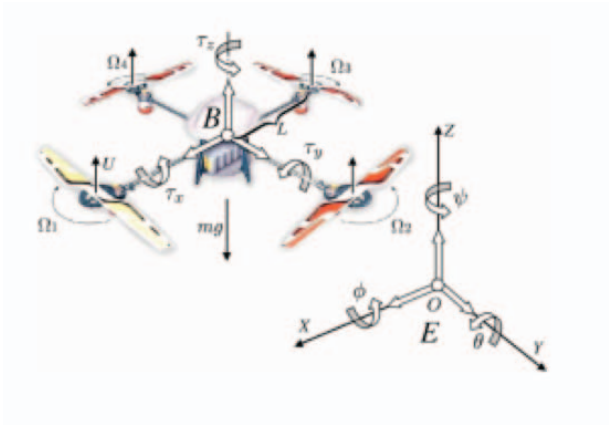

Fig. 2: Coordinate system for quadrotor modeling. Source: extracted from [6].

According to [7], the dynamics of a quadrotor may be derived from classical mechanics equations for linear and angular momenta and resembles like the following:

$$\ddot{x} = (cos\phi \cdot sin\theta \cdot cos\psi + sin\phi \cdot sin\psi) \cdot \frac{1}{m} \cdot u_1 \quad (1)$$

$$\ddot{y} = (cos\phi \cdot sin\theta \cdot sin\psi - sin\phi \cdot cos\psi) \cdot \frac{1}{m} \cdot u_1 \quad (2)$$

$$\ddot{z} = -g + (cos\phi \cdot cos\theta) \cdot \frac{1}{m} \cdot u_1 \quad (3)$$

$$\ddot{\phi} = \dot{\theta} \cdot \dot{\psi} \cdot \frac{I_y - I_z}{I_x} + \frac{u_2}{I_x} \quad (4)$$

$$\ddot{\theta} = \dot{\phi} \cdot \dot{\psi} \cdot \frac{I_z - I_x}{I_y} + \frac{u_3}{I_y} \quad (5)$$

TABLE I: Description os symbols and parameters.

Symbol	Definition
x	x-coordinate position
y	y-coordinate position
z	z-coordinate position
θ	roll angle
ϕ	pitch angle
ψ	yaw angle
g	gravity acceleration
d	drag coefficient of propellers
b	upthrust coefficient
l	length of rods
$u_1...u_4$	control signals
$\Omega_1...\Omega_4$	velocity of actuators
I_x, I_y, I_z	rotational inertia
m	vehicle's mass

$$\ddot{\psi} = \dot{\phi} \cdot \dot{\theta} \cdot \frac{I_x - I_y}{I_z} + \frac{u_4}{I_z} \quad (6)$$

A brief description for every term present in the above and in the upcoming equations is provided in Table I.

Equation (1)-(3) show that the horizontal (in-plane) or vertical (along z-axis) displacement of a quadrotor is a function of the yaw, pitch and roll angles. The control signals $u_1....u_4$ appearing in equations (1)-(6) above represent torque and, as such, have a direct relation to the geometrical measurements of the equipment, as well as to the velocity of the motors, as reported in equations (7)-(10) below. We emphasize this formulation follows [8].

$$u_1 = b \cdot \left(\Omega_1^2 + \Omega_2^2 + \Omega_3^2 + \Omega_4^2\right) \quad (7)$$

$$u_2 = b \cdot l \cdot \left(\Omega_4^2 - \Omega_2^2\right) \quad (8)$$

$$u_3 = b \cdot l \left(\Omega_1^2 - \Omega_3^2\right) \quad (9)$$

$$u_4 = d \cdot \left(\Omega_4^2 + \Omega_2^2 - \Omega_3^2 - \Omega_1^2\right) \quad (10)$$

III. Cascade PID strategy

For what concerns the control strategy adopted, the PID alternative was chosen because it is a kind of universal and widely spread approach for quadrotors (see, for instance, [1], [8], [7] and references therein). For reference the PID control law for the inputs $u_1...u_4$ is reported in the following:

$$u_i = K_p \cdot e(t) + K_i \cdot \int_0^t e(\tau)d\tau + K_d \cdot \frac{de(t)}{dt} \quad (11)$$

where $e(t)$ is the difference between desired and actual measurement, and K_p, K_i, K_d constitute a set of proportional, integrative and derivative constants for the gain actions. The rotational speed of each motor is then obtained by inverting equations (7)-(10) and solving for $\Omega_1...\Omega_4$:

$$\Omega_1^2 = \frac{u_1}{4 \cdot b} - \frac{u_3}{2 \cdot b \cdot l} - \frac{u_4}{4 \cdot d} \quad (12)$$

$$\Omega_2^2 = \frac{u_1}{4 \cdot b} - \frac{u_2}{2 \cdot b \cdot l} + \frac{u_4}{4 \cdot d} \tag{13}$$

$$\Omega_3^2 = \frac{u_1}{4 \cdot b} + \frac{u_3}{2 \cdot b \cdot l} - \frac{u_4}{4 \cdot d} \tag{14}$$

$$\Omega_4^2 = \frac{u_1}{4 \cdot b} + \frac{u_2}{2 \cdot b \cdot l} + \frac{u_4}{4 \cdot d} \tag{15}$$

The closed-loop system for position, attitude and height control used cascaded PID controllers as depicted in Figure 3, which is in accordance to [6].

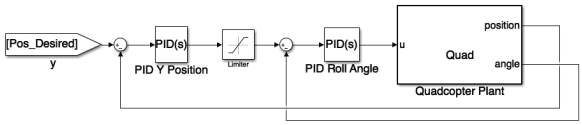

Fig. 3: Cascade PID strategy for y-axis positioning.

In Figure 3 two control loops are present. The inner loop is responsible for angle correction and it has to be faster than the external one because the attitude control is more critical for flight stabilization than the position control. The external loop, in turn, is responsible for horizontal positioning (in xy-plane). The whole control system should, therefore, consider the horizontal and vertical coordinates, as well as the orientation angles. One solution for that is the use of six PID control loops whose interdependence is illustrated in Figure 4.

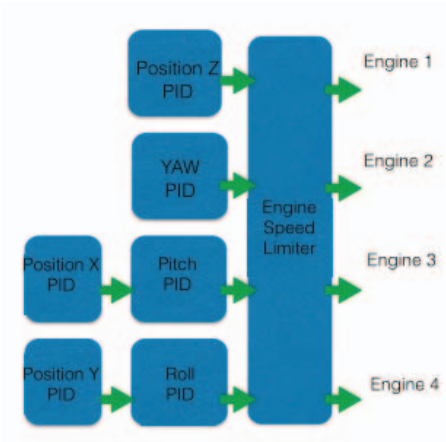

Fig. 4: Cascade PID strategy for the whole system control.

IV. Control Validation

With the purpose of illustrating the proposed control architecture, we considered the hypothetical situation of a navigation starting at point $(x = 0, y = 0, z = 0)$ and ending at $(x = 1, y = 1, z = 1)$. Simulation results for this test are reported in Figure 5 below.

It is worth mentioning that in this analysis we applied the small-variation approximation for the orientation angles,

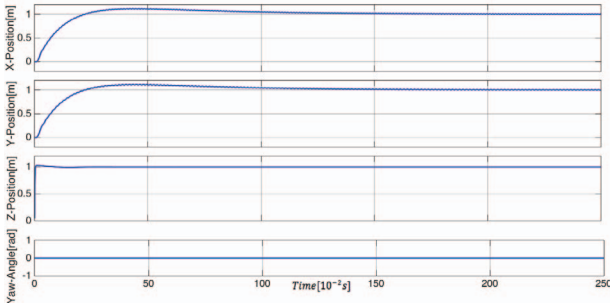

Fig. 5: Dynamic response of the quadrotor after unitary step positioning in three spatial coordinates.

therefore ψ, ϕ and $\theta \approx 0$. This assumption allows for decoupling equations (1)-(6), which can be rewritten as:

$$\ddot{x} = \theta \frac{1}{m} \cdot u_1 \tag{16}$$

$$\ddot{y} = -\phi \frac{1}{m} \cdot u_1 \tag{17}$$

$$\ddot{z} = -g + \frac{1}{m} \cdot u_1 \tag{18}$$

$$\ddot{\phi} = \frac{u_2}{I_x} \tag{19}$$

$$\ddot{\theta} = \frac{u_3}{I_y} \tag{20}$$

$$\ddot{\psi} = \frac{u_4}{I_z} \tag{21}$$

Although this assumption is crucial for the quarotor control, it limits the validity of the dynamic equations to well-behaved environments. In other words, the model fails when the environment has such strong wind patterns, in which the null-variation of orientation angle is no longer reasonable.

V. Reduced Attitude Study

A. Performance of PID under motor failure

With the aim to investigate how the PID control performs under motor-failure, we simulated the scenario of breaking of 2 opposite motors. Here is the procedure: 1) the working UAV was initially placed at $(x = 0, y = 0, z = 0)$ coordinates; 2) then it raised up to $z = 1$ meters above ground; 3) after that, two opposite motors were forced to zero rotational speed; 4) the setpoints of the angles *roll* and *pitch* were set to zero and ignored horizontal position errors; 5) finally, the dynamic time-series of position and orientation variables were recorded for investigation. This methodology was inspired on the very recent contribution of [4]. The results of this test are plot in Figure 6.

From Figure 6, it can be seen there is numerical divergence on the position control along x-axis and y-axis, but vertical control is still achieved. This can be associated to the appearance of a rotation around z-axis, what makes the orientation

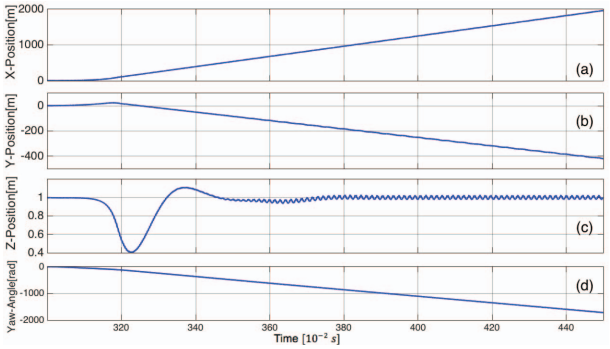

Fig. 6: Dynamic response of the quadrotor after breaking of 2 motors.

angles to be coupled. To see this, note that, for a working and stabilized quadrotor, $u_4 = 0$. Also, check out how equation (10) influences equation (6) when $\Omega_2 = \Omega_4 = 0$. Such a coupling is the reason why the single-input/single-output PID approach used so far fail and, since $\dot{x}$ and $\dot{y}$ will now depend on θ and ϕ in equation (1), a multivariable control is recommended.

Although a number of papers discuss the flight stabilization even with 1 or 2 motors lost, the solution usually comes at the expense of a robust controller design, as the linear-quadratic regulator (LQR) of [4] and [5]. The study of this strategy is left for future work, because our present interest is to understand whether the PID can be adopted as critical controller.

B. Influence of geometrical design

A look at Figure 6d reveals that the quadrotor spins around z-axis when two motors-failure occurs. Since now the dynamic equations get coupled, the increase in the magnitude of ψ leads to monotonic increase in position around y-axis and x-axis as well. Furthermore, uncertainty on z-axis position appears (see Figure 6c). A natural question to be made at this moment is how to mitigate this phenomenon. Is it possible to keep the rotational speed around z-axis at acceptable levels in such a way the small-variation assumption still holds? Is it possible to reduce the fluctuation observed in the vertical position?

Well, the second issue studied in this paper is the influence of the geometrical design of the UAV on its navigation condition under failure. According to [9], the drag force is related to the shape, velocity and material properties of the object of interest. For rotational movement, like that of a quadrotor, the aerodynamic drag represents a resistance torque, which is, according to [4], dependent on the rotational speed. This proportionality is expresses as $\frac{-\gamma \cdot \dot{\psi}}{I_z}$. in which γ is a drag coefficient in N.m.s. This term can be added to equation (6), which now resembles like:

$$\ddot{\psi} = -\frac{\gamma \cdot \dot{\psi}}{I_z} + \dot{\phi} \cdot \dot{\theta} \frac{I_x - I_y}{I_z} + \frac{u_4}{I_z} \tag{22}$$

A look at equation (22) shows that the smaller γ is, the faster the spin movement around the z-axis will be. The solution of the dynamic equations reveals that, in this scenario of reduced drag coefficient the uncertainty in the vertical position decreases as well. Therefore, the route to precisely lock the z-coordinate of the reduced attitude quadrotor is to look for a suitable geometrical design presenting low aerodynamic drag.

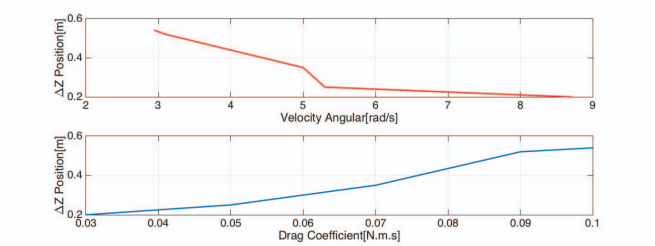

Fig. 7: Influence of the drag coefficient on the vertical position uncertainty.

In the results presented in Figure 7, the lower bound of 0.03 N.m.s represents the limit case under which we face numerical problems to solve the dynamics.

To partially answer the motivation questions, we considered two different geometries for the rods, one with circular and the other with square cross-section. By applying the drag formula, we found the cylindrical rods present smaller drag force. To make a fair comparison, considere a spin velocity of -3 rad/s and a rod with 0.03 m x 0.03 m x 0.6 m rectangular profile, as well as another rod with cylindrical profile of the same length (0.6 m) and having cross-section diameter equal to 0.03 m. In this case, the cylindrical shape offers a 1.3 times higher drag.

This discussion makes clear that quadrotors with cylindrical shaped rods will present less fluctuation on vertical position when attitude reduced.

C. Fail-safe technique

Aware of the fact that the horizontal positioning is no longer possible (the vehicle flights away, according to simulations) and in order to prevent damages and accidents it is recommended the quadrotor be landed. We point-out that the shorter the time required to reach the ground, the smaller will be the horizontal deviation from the original position just before breaking. To accomplish with this requirements, we propose an algorithm able to detect the fail and switch to the critical controller, as described by the following steps:

1) the fail-safe strategy is triggered whenever the rotational speed around z-axis gets over -2 rad/s; 2) then roll and pitch angles are set to zero, thus we disregard the horizontal position error of the loop control. This change in the control loop of roll may be seen in Figure 8; 3) the setpoint for height control is dinamically changed according to an exponential decaying function.

In the above strategy, step 2 is necessary to prioritize the attitude of stability, which prevent flipping that would turn

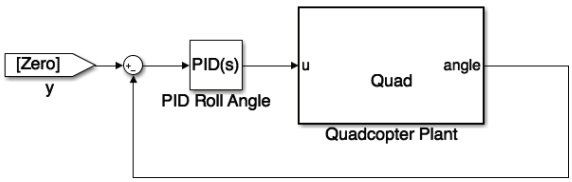

Fig. 8: PID strategy for roll angle after breaking of 2 motors.

the landing into a impossible task. On the other hand, step 3 is necessary to guarantee convenient landing in the vicinity of the region where the failure took place, in such a way the ground approaching velocity be near zero.

We simulated the above algorithm and the results are presented in Figure 9 and 10. The vehicle was initially in working conditions and, then, at time instante $t = 300$ s we switched-off two motors by forcing $\Omega_2 = \Omega_4 = 0$ in equations (7)-(10). From Figure 9, we see the quadrotor initially at $z = 1$m and, after the peak in vertical velocity due to the trigger of the reduced attitude scenario, it is decelerated, smoothly reaching the ground 4 seconds later.

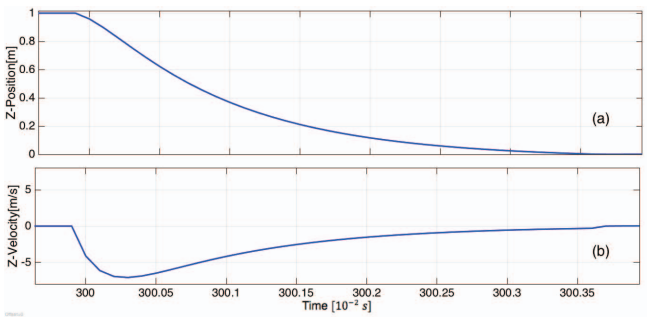

Fig. 9: Dynamic simulation of near-vertical landing when fail-safe is on.

As already mentioned, the rapidity of such an exponential decay is essential to limit the horizontal deviation when the quadrotor starts flighting away. To investigate that, in Figure 10 we plot the horizontal deviation as a function of different time constants of the exponential vertical trajectory. The region of interest is the lower-left part of the graph, which means, in practice, a completely vertical landing.

VI. Preliminary Results

In order to evaluate the results obtained from simulations of a quadrotor in failure regime, started up experiments using a real quadcopter. The first test was realized with the purpose of observing the emergence of the a rotation around the axis z and the altitude variation with the loss of two opposite motors. For that, we used the following methodology: 1) qudrotor was put at an altitude of 1.8 m; 2) later, two opposing engines were shut down abruptly; 3) after the loss of the engines, the setpoints of the angles *roll* and *pitch* were set to zero and ignored horizontal position errors; 4) All

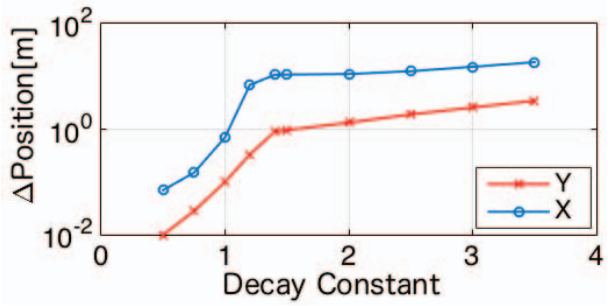

Fig. 10: Influence of the decay rate of the exponential trajectory on the horizontal position deviation.

data from the accelerometer, gyroscope and other sensors embedded in the experimental platform were sent via radio frequency to a computer responsible for storage. Thus, the Figure 11 was generated.

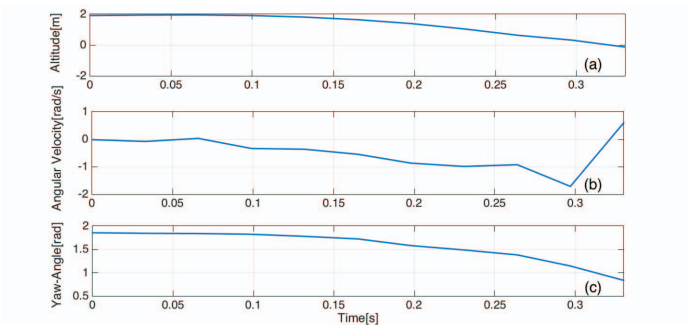

Fig. 11: Dynamic behavior exhibited by real quadrotor in the first test.

In Figure 11, there is the altitude loss of the quadcopter given by Figure 11(a), it happens, because the two running motors do not generate sufficient thrust to support this equipment. Too view, in Figure 11(b) the appearance of a rotation around the z axis and hence growth a negative angle yaw in Figure 11(c). This behavior is originated by engines that rotate clockwise.

As mentioned, the quadcopter involved in the trials failed to maintain its altitude, thus opted for the use of a support of sustaining, consists of a pulley and a nylon line connected to center of mass of the equipment. This strategy was designed for enable the visualization of the dynamic behavior of the quadrotor, if the two remaining engines, after the failure could sustain it. Therefore, the results obtained with this new strategy and using the same methodology as the previous experiment, was conceived to Figure 12.

From Figure 12, after the failure of the engines, there is the appearance of a rotation around the z axis, which becomes constant due to drag of structure that compensate the resultant torque of the engines running. Thus, the angular acceleration in the z axis approaches zero, the angular velocity becomes constant, see Figure 12(b), and the yaw angle tends to infinity, Figure 12(c).

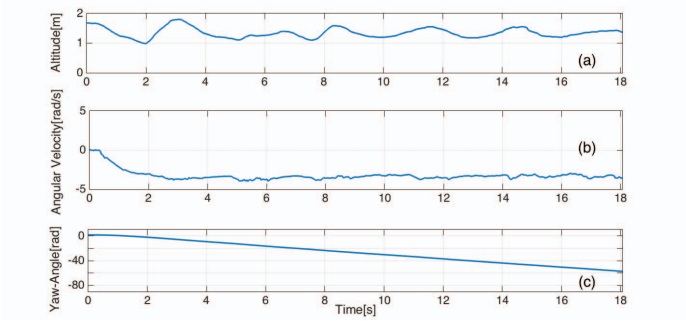

Fig. 12: Dynamic behavior exhibited by real quadcopter in the second test.

After the initial tests, it was found that the dynamic behavior seen in the simulations, see Figure 6(c) and 6(d), were similar to those presented by the actual quadcopter, see Figure 12(a) and 12(c), respectively. Thus validating the modeling presented herein. It is important highlight that the objective this work is not to create a identical mathematical model to reality, but of conceiving simulations that show the approximate dynamic behavior of a real quadrotor.

VII. Conclusions

In this paper we addressed the issue of flight stabilization control in reduced attitude unmanned quadrotor. From numerical simulations we explained that the PID strategy itself is not effective to guarantee safe navigation after a two-engine fail occurs. Nevertheless, we showed the PID strategy can be adopted if a fail-safe technique approach is promply triggered after the failure. To accomplish with that, a fail-safe algorithm has been proposed and used to investigate, from simulations, how the vehicles' flight perform when it is on and how the quadrotor flights away whenever it is kept off.

The flighting away scenario has further been investigated by looking at geometrical design issues of the UAV. In this regard we showed that the horizontal flight deviation is suppressed whenever the aerodynamic drag is kept at low leves, what is favoured by the adoption of cylindrical shaped rods. For what concerns the fail-safe performance, in turn, our approach consists in forcing a exponential-like trajectory control along z-coordinate and results suggest that the decay rate of the trajectory has to be made as fast as possible to ensure an almost-vertical and safe landing after failure, with near zero velocity on ground approaching.

VIII. Futures Works

As futures works: 1) we are embedding the proposed algoritm into the UAV of Figure 1 and the performance of experimental tests; 2) we will accomplish the theoretical evidence concerning the influence of geometry of quadcopter on the fault condition presented here; 3) the Analysis of stability with critical controller; 4) and the theoretical proof of the influence of drag coefficient on the variation of altitude of the Quadcopter in fault regime, which can be done from the influence of theta and phi in the equation (3) and psi in the angular accelerations around the x-axis, equation (4), and y-axis, equation (5).

Acknowledgement

Authors acknowledge CAPES for financial support and Fundação NUTEC, for administrative facilities.

References

[1] R. C. Sá, "Dynamic modeling, implementation and pid control for stability of a quadrotor-type unmanned aerial vehicle," Master's thesis, Master of Science in Engenharia de Teleinformática-Universidade Federal do Ceará, Fortaleza, 2012.

[2] F. R. G. Lippielo and D. Serra, "Emergency landing for a quadrotor in case of a propeller failure: A backstepping approach," in *Proceedings of the IEEE/RSJ International Conference on Intelligent Robots and Systems*. IEEE, 2014, pp. 4782–4788.

[3] M. Ranjbaran and K. Khorasani, "Fault recovery of an under-actuated quadrotor aerial vehicle," in *Proceedings of the 49th IEEE Conference on Decision and Control*. IEEE, 2010, pp. 4385–4392.

[4] M. W. Mueller and R. DAndrea, "Stability and control of a quadrocopter despite the complete loss of one, two, or three propellers," in *Proceedings of the IEEE International Conference on Robotics and Automation (ICRA 2014)*. IEEE, 2014, pp. 45–52.

[5] A. F. A. Lanzon and S. Longhi, "Flight control of a quadrotor vehicle subsequent to a rotor failure," *Journal of Guidance, Control, and Dynamics*, vol. 37, no. 2, pp. 580–591, 2014.

[6] P. H. Q. A. Santana and G. A. Borges, "Modelagem e controle de quadrirotores," in *Proceedings of the Simpósio Brasileiro de Automação Inteligente (SBAI 2009)*, 2009, pp. 1–6.

[7] T. Jiřinec, "Stabilization and control of unmanned quadcopter," Master's thesis, Master of Science in Space Engineering-Czech Technical University, Prague, 2011.

[8] M. A. R. Al-Omari, "Integrated simulation platform for indoor quadrotor applications," in *Proceedings of the 9th International Symposium on Mechatronics and its Applications (ISMA13)*, 2013, pp. 1–6.

[9] S. Maxemow, "That's a drag: The effects of drag forces," *Undergraduate Journal of Mathematical Modeling: one + two*, vol. 2, no. 1, p. article 4, 2009.